

AD-A192 025

THE INFLUENCE OF UNCOMPENSATED SOLUTION RESISTANCE ON
THE DETERMINATION A. (U) PURDUE UNIV LAFAYETTE IN DEPT
OF CHEMISTRY D F MILNER ET AL. 25 SEP 87

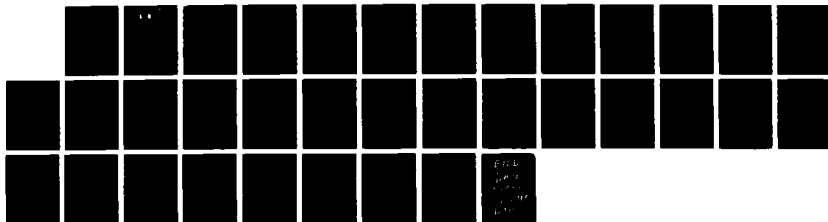
1/1

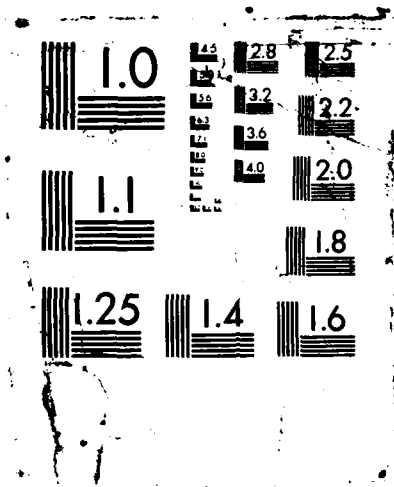
UNCLASSIFIED

N00014-86-K-0556

F/G 7/4

NL





DTIC FILE COPY

①

SECURITY

AD-A192 825 DOCUMENTATION PAGE

1a REP Unclassified			1b RESTRICTIVE MARKINGS		
2a SECURITY CLASSIFICATION AUTHORITY SELECTED MAR 25 1988			3 DISTRIBUTION / AVAILABILITY OF REPORT Approved for public release and sale; its distribution is unlimited.		
2b DECLASSIFICATION / DOWNGRADING SCHEDULE			5 MONITORING ORGANIZATION REPORT NUMBER(S)		
4 PERFORMING ORGANIZATION REPORT NUMBER(S) Technical Report No. 68			7a NAME OF MONITORING ORGANIZATION Division of Sponsored Programs Purdue Research Foundation		
6a NAME OF PERFORMING ORGANIZATION Purdue University Department of Chemistry		6b OFFICE SYMBOL (If applicable)	7b ADDRESS (City, State, and ZIP Code) Purdue University West Lafayette, Indiana 47907		
6c ADDRESS (City, State, and ZIP Code) Purdue University Department of Chemistry West Lafayette, Indiana 47907		9 PROCUREMENT INSTRUMENT IDENTIFICATION NUMBER Contract No. N00014-86-K-0556			
8a NAME OF FUNDING / SPONSORING ORGANIZATION Office of Naval Research		8b OFFICE SYMBOL (If applicable)	10 SOURCE OF FUNDING NUMBERS		
8c ADDRESS (City, State, and ZIP Code) 800 N. Quincy Street Arlington, VA 22217		PROGRAM ELEMENT NO	PROJECT NO	TASK NO	WORK UNIT ACCESSION NO
11 TITLE (Include Security Classification) The Influence of Uncompensated Solution Resistance on the Determination and Standard Electrochemical Rate Constants Using Cyclic Voltammetry, and Some Comparisons with AC Voltammetry					
12 PERSONAL AUTHOR(S) D. F. Milner and M. J. Weaver					
13a TYPE OF REPORT Technical		13b TIME COVERED FROM 10/1/86 TO 9/30/87		14 DATE OF REPORT (Year, Month, Day) September 25, 1987	
15 PAGE COUNT					
16 SUPPLEMENTARY NOTATION					
17 COSATI CODES			18 SUBJECT TERMS (Continue on reverse if necessary and identify by block number)		
FIELD	GROUP	SUB-GROUP	digital simulation analysis, uncompensated solution resistance, electrochemical rate constants, cyclic voltammetry		
19 ABSTRACT (Continue on reverse if necessary and identify by block number) A digital simulation analysis is presented of the deleterious effects of uncompensated solution resistance, R_{us} , upon the evaluation of standard rate constants, $k_{ob}^{2,7}$, using cyclic voltammetry. The results are expressed in terms of systematic deviations of "apparent measured" rate constants, $k_{ob}^{2,7}(app)$, evaluated in the conventional manner without regard for R_{us} , from the corresponding actual values, $k_{ob}^{2,7}(true)$, as a function of R_{us} and other experimental parameters. Attention is focused on the effects of altering the electrode area and the double-layer capacitance upon the extent of the deviations between $k_{ob}^{2,7}(app)$ and $k_{ob}^{2,7}(true)$, and on comparisons with corresponding simulated results obtained from phase-selective ac impedance data. The extent to which $k_{ob}^{2,7}(app) < k_{ob}^{2,7}(true)$ for small R_{us} values was found to be similar for the cyclic and ac voltammetric techniques. The latter method is, however, regarded as being preferable under most circumstances in view of the greater ease of minimizing, as well as evaluating, R_{us} for ac impedance measurements. The influence of solution resistance on $k_{ob}^{2,7}$ measurements using microelectrodes and without iR compensation is also considered.					
20 DISTRIBUTION / AVAILABILITY OF ABSTRACT <input checked="" type="checkbox"/> UNCLASSIFIED/UNLIMITED <input checked="" type="checkbox"/> SAME AS RPT <input type="checkbox"/> DTIC USERS			21 ABSTRACT SECURITY CLASSIFICATION Unclassified		
22a NAME OF RESPONSIBLE INDIVIDUAL			22b TELEPHONE (Include Area Code)		22c OFFICE SYMBOL

→ Keynotes

OFFICE OF NAVAL RESEARCH

Contract N00014-86-K-0556

Technical Report No. 68

The Influence of Uncompensated Solution Resistance on the
Determination and Standard Electrochemical Rate Constants
Using Cyclic Voltammetry, and Some Comparisons with AC Voltammetry

by

D. F. Milner and M. J. Weaver

Prepared for Publication

in the

Anal. Chim. Acta

198, 245-57 (1987)

Purdue University

Department of Chemistry

West Lafayette, Indiana 47907

September 25, 1987



Accession For	
NTIS	CRA&I
DTIC	TAB
Unannounced	
Justification	
By	
Distribution	
Availability Codes	
Dist	Availability for Special
A-1	

Reproduction in whole, or in part, is permitted for any purpose of the United States Government.

* This document has been approved for public release and sale: its distribution is unlimited.

88 3 22 091

The Influence of Uncompensated Solution Resistance on
the Determination of Standard Electrochemical Rate Constants
Using Cyclic Voltammetry, and Some Comparisons with AC Voltammetry

David F. Milner and Michael J. Weaver
Department of Chemistry, Purdue University,
West Lafayette, Indiana 47907, U.S.A.

ABSTRACT

A digital simulation analysis is presented of the deleterious effects of uncompensated solution resistance, R_{us} , upon the evaluation of standard rate constants, k_{ob}^s , using cyclic voltammetry. The results are expressed in terms of systematic deviations of "apparent measured" rate constants, $k_{ob}^s(app)$, evaluated in the conventional manner without regard for R_{us} , from the corresponding actual values, $k_{ob}^s(true)$, as a function of R_{us} and other experimental parameters. Attention is focused on the effects of altering the electrode area and the double-layer capacitance upon the extent of the deviations between $k_{ob}^s(app)$ and $k_{ob}^s(true)$, and on comparisons with corresponding simulated results obtained from phase-selective ac impedance data. The extent to which $k_{ob}^s(app) < k_{ob}^s(true)$ for small R_{us} values was found to be similar for the cyclic and ac voltammetric techniques. The latter method is, however, regarded as being preferable under most circumstances in view of the greater ease of minimizing, as well as evaluating, R_{us} for ac impedance measurements. The influence of solution resistance on k_{ob}^s measurements using microelectrodes and without iR compensation is also considered.

In recent years cyclic voltammetry (CV) has been utilized to determine standard electrochemical rate constants, k^s , for a great number of redox couples under widely varying conditions. The rate constants have been most commonly derived from the cyclic voltammograms by using the Nicholson-Shain type of analysis,¹ although other methods have also been employed.² Particularly given the common and sometimes indiscriminant use of CV for this purpose, it is important to ascertain clearly the range of system properties and measurement conditions over which the observed rate parameters are indeed valid. This is of particular concern when relatively rapid rate constants are required to be evaluated, since the effect of even small positive amounts of uncompensated resistance, R_{us} , can easily be misinterpreted as slow electrode kinetics under these conditions.^{1a} In addition to the deleterious influence of solution resistance, measurement nonidealities associated with the effects of potentiostat bandwidth and double-layer charging current also need to be considered.

Digital simulations of cyclic voltammograms of varying complexity have been performed for as long as cyclic voltammetry has been employed for evaluating k^s for quasireversible systems.^{1,3} These simulations have primarily been of the "idealized" form³ in which no instrumental or electrochemical artifacts, such as arising from R_{us} , the double-layer capacitance C_{dl} , or finite amplifier bandwidths, are considered to affect the cell response. Although significant attention has been given to the development of algorithms which account for the influence of R_{us} upon the cyclic voltammograms,⁴ surprisingly little effort has been directed towards providing analyses which enable the experimentalist to readily deduce the consequences for the reliable measurement of k^s . A significant difficulty

is that the solution resistance distorts cyclic voltammograms in a manner qualitatively similar to that of sluggish electrode kinetics.^{1a} This can produce considerable uncertainty in evaluating the latter in the presence of the former, especially for moderate or large k^s values ($> 10^{-2} \text{ cm s}^{-1}$). While it is usual to employ positive-feedback compensation so to minimize R_{us} , it is extremely difficult to reduce R_{us} to zero without severely distorting the potential-time ramp applied to the cell.⁵

By means of digital simulations we have recently examined the combined influence of uncompensated solution resistance and other measurement nonidealities on the determination of k^s by means of ac impedance techniques.⁶ For this purpose it was found useful to distinguish between "apparent" observed rate constants, $k_{ob}^s(\text{app})$, that are obtained for a given instrument and measurement conditions by means of the conventional analysis assuming such nonidealities to be absent, and the desired actual ("true") value of the rate constant, $k_{ob}^s(\text{true})$. The extent of the systematic deviations between $k_{ob}^s(\text{app})$ and $k_{ob}^s(\text{true})$ was examined as a function of R_{us} and the magnitude of $k_{ob}^s(\text{true})$ in order to provide means by which the reliability of the $k_{ob}^s(\text{app})$ values could be diagnosed, and to enable the extent of the corrections to $k_{ob}^s(\text{app})$ arising from the presence of measurement nonidealities to be determined.⁶

The present communication summarizes the results of a comparable digital simulation study aimed at assessing the reliability of $k_{ob}^s(\text{app})$ values obtained by using cyclic voltammetry. Of particular interest is the extent to which the presence of uncompensated solution resistance provides an effective upper limit to the reliable evaluation of $k_{ob}^s(\text{true})$ for a given set of measurement conditions, and how this limit for cyclic

voltammetry compares to that for corresponding ac impedance measurements. Simulation parameters are chosen so to correspond to a range of conditions appropriate to typical aqueous and nonaqueous media. The effect of varying the electrode area is considered, including conditions appropriate for microelectrodes.

SIMULATION PROCEDURES

The digital simulations of cyclic voltammograms performed in this study were of two types. For those instances where the effect of C_{dl} was not considered, the method of Nicholson^{4a} was used, while those where this influence was included were finite difference simulations similar to those described by Feldberg.³

The values of the various system parameters employed in the simulations were selected to be representative of those commonly encountered for redox couples in nonaqueous solvents as well as aqueous media. The ranges of R_{us} values chosen ($< 50 \text{ ohm}$) are based on the minimum values that we have generally been able to obtain in studies utilizing common commercial potentiostats, such as the PAR 173/179 system (vide infra). The reactant (and product) diffusion coefficient was taken to be $1 \times 10^{-5} \text{ cm}^2 \text{ s}^{-1}$, the electrochemical transfer coefficient was assumed to equal 0.5, the number of electrons transferred, n , equals one, and the reactant concentration was taken to be 1 mM unless otherwise noted. The voltammetric sweep rate was set at 20 V s^{-1} unless specified otherwise.

The general procedure involved simulating cyclic voltammograms for a suitable range of system input parameters, including $k_{ob}^s(\text{true})$ and R_{us} values, and extracting "apparent observed" rate constants, $k_{ob}^s(\text{app})$, from

the simulated voltammetric curves in the same fashion as is conventional for experimental data. For simplicity, this involved evaluating $k_{ob}^s(app)$ from the difference between the cathodic and anodic peak potentials, ΔE_p , using $\Delta E_p - \psi$ plots in the manner prescribed by Nicholson.^{1a} Where necessary, simulations were performed under "ideal" conditions (i.e. for $R_{us}, C_{dl} = 0$) so to generate more complete $\Delta E_p - \psi$ data and thereby avoid any interpolation errors encountered by using Table I of ref. 1a. Strict adherence was also paid to the potential scan limits specified for the validity of the $\Delta E_p - \psi$ relation in ref. 1a.

All simulation programs were written in FORTRAN-77 and executed on a DEC LSI 11-73 microcomputer under the RSX11-M operating system.

RESULTS AND DISCUSSION

Origins of Distortion of Cyclic Voltammograms from Uncompensated Solution Resistance

Before examining systematically the extent to which the presence of R_{us} can lead to systematic differences between $k_{ob}^s(app)$ as determined by cyclic voltammograms and the required $k_{ob}^s(true)$ values, it is useful to clarify the origins of the underlying distortions in the current-potential profiles. Under most conditions, the solution resistance will be incompletely compensated by the potentiostat positive-feedback circuitry so that R_{us} will be positive. The presence of R_{us} will yield a net ohmic potential drop, iR_{us} , through the solution in proportion to the current, i , flowing. Since the current peaks for the negative- and positive-going potential sweeps have opposite signs, the measured cathodic-anodic peak separation, ΔE_p , will clearly be larger for positive R_{us} than the "ideal"

case, where $R_{us} = 0$.

An additional, less obvious, source of distortion arises from the fact that when $R_{us} \neq 0$ only the time derivative of the overall cell potential, dE_{cell}/dt , will be held constant during the voltammetric scan, rather than the corresponding derivative of the double-layer potential, dE_{dl}/dt , as is required for the exact applicability of the usual CV treatment. As a consequence, dE_{dl}/dt will vary with E_{cell} so to distort the measured ΔE_p still further in the presence of R_{us} . This is illustrated in Fig. 1, which shows simulated $i - E_{cell}$ and $(dE_{dl}/dt) - E_{cell}$ traces for a negative-going potential sweep, with $(dE_{cell}/dt) = \nu = 100 \text{ V s}^{-1}$. The electrode area, A , is taken as 0.2 cm^2 , R_{us} as 50 ohms, and C_{dl} as $20 \mu\text{F cm}^{-2}$. The magnitude of dE_{dl}/dt is such that it is less negative when i is decreasing (Fig. 1b). This "acceleration" of the effective sweep rate in the vicinity of the current peak contributes to larger ΔE_p values than in the absence of uncompensated solution resistance.

The nonfaradaic current, i_{nf} , resulting from nonzero C_{dl} values will also contribute to this distortion. This is because i_{nf} enhances the total current throughout the voltammogram, and therefore further enlarges ΔE_p than when $R_{us} = 0$. This capacitive contribution to ΔE_p , $\Delta(\Delta E_p)$, can be determined approximately from $\Delta(\Delta E_p) = 2 C_{dl} R_{us} \nu$, where ν is the applied potential scan rate (dE_{cell}/dt). However, the precise influence of C_{dl} upon ΔE_p will be more complex, not only because C_{dl} is usually potential dependent, but also since the scan rate ν in this relation should really be identified with (dE_{dl}/dt) rather than with (dE_{cell}/dt) .

Influence of Varying the Uncompensated Solution Resistance on the Cyclic Voltammetric Determination of k_{ob}^s

It is well known that the presence of R_{us} can lead to large systematic errors in the determination of k_{ob}^s , since increasing R_{us} or decreasing k_{ob}^s both lead to greater ΔE_p values under a given set of experimental conditions.^{1a} A common procedure is to "fit" the experimental current-potential curves to corresponding simulated curves obtained for a set of input parameters and trial k_{ob}^s values until the best match is obtained.^{2c,7} Although this procedure is in a sense preferable to the examination of ΔE_p values alone, it is not always obvious that obtaining a "good fit" of the simulated to the experimental data is due to the correctness of the choice of k_{ob}^s rather than to an incorrect choice of other system variables, especially R_{us} .

The crux of the problem is that the diagnosis of ΔE_p values greater than the "reversible" limit (i.e. for $k_{ob}^s \rightarrow \infty$), $(59/n)\text{mV}$ at 25°C , as arising purely from the presence of "finite" (i.e. measurable) k_{ob}^s values rather than at least partly from $R_{us} > 0$ is far from straightforward. For example, Fig. 2 shows a pair of simulated cyclic voltammograms, the points corresponding to $k_{ob}^s = 0.04 \text{ cm s}^{-1}$ and $R_{us} = 0$, and the solid trace referring to $k_{ob}^s = \infty$ and $R_{us} = 50 \text{ ohm}$. (The latter value is chosen here since it approximates the magnitude of R_{us} that can be anticipated in many nonaqueous media.⁸) The close similarity in the two curves, in addition to the almost identical ΔE_p values, clearly make the evaluation of k_{ob}^s values even as small as 0.04 cm s^{-1} fraught with difficulty unless R_{us} is known accurately, or preferably diminished substantially below 50 ohm . Although it is common to examine the dependence of ΔE_p on the sweep rate, ν , in

order to evaluate k_{ob}^s , this procedure provides little or no diagnosis for the dominant presence of finite electrode kinetics rather than R_{us} since both show a similar $\Delta E_p - \nu$ dependence.^{1a} This is illustrated in Fig. 3, which shows plots of ΔE_p against ν for the same conditions as in Fig. 2. Both the resistance-dominated (solid curve) and kinetics-dominated (squares) plots are almost indistinguishable. Clearly, then, substantial systematic errors in the evaluation of k_{ob}^s , so that $k_{ob}^s(app) < k_{ob}^s(true)$, can occur for analyses of this type unless R_{us} is known accurately.

In principle, a distinction between resistive- and kinetically-dominated ΔE_p behavior can be obtained by varying the bulk reactant concentration, C_b , while holding all other parameters fixed.⁸ As shown in Fig. 4, if the sweep-rate dependent ΔE_p is dominated by R_{us} , then ΔE_p should increase roughly linearly with C_b , whereas ΔE_p will be independent of C_b if the ΔE_p response is dominated by sluggish kinetics, at least if these are first order so that k_{ob}^s is independent of C_b . This approach, however, is often not a practical one. In circumstances where either positive-feedback iR compensation and/or a Luggin probe is used to minimize R_{us} it is usually very difficult to maintain precisely the same R_{us} values on successive measurements using solutions of varying reactant concentration. Moreover, the presence of nonfaradaic current leads to some influence of R_{us} upon ΔE_p even when $C_b \rightarrow 0$ (Fig. 4). Consequently, it is difficult to use this strategy to diagnose the influence of R_{us} upon the cyclic voltammograms except under relatively favorable circumstances.

It is therefore apparent that an accurate knowledge of R_{us} is a prerequisite for the reliable determination of k_{ob}^s by means of cyclic voltammetry. As noted above, we have previously utilized digital

simulations to examine deviations between $k_{ob}^s(\text{true})$ and $k_{ob}^s(\text{app})$ as a function of R_{us} for ac impedance measurements, where $k_{ob}^s(\text{app})$ is determined from the conventional analysis that assumes that $R_{us} = 0$.⁶ Such relationships enable estimates of $k_{ob}^s(\text{true})$ to be obtained from measured $k_{ob}^s(\text{app})$ values if R_{us} is known, as well as providing an upper limit to the $k_{ob}^s(\text{app})$ values for which meaningful kinetic information can be extracted.

Examples of such relationships obtained for cyclic voltammetry are shown in Figs. 5 and 6 in the form of plots (solid curves) of $\log k_{ob}^s(\text{app})$ versus R_{us} for various $k_{ob}^s(\text{true})$ values. The $k_{ob}^s(\text{app})$ values were obtained from the ΔE_p values for simulated cyclic voltammograms by using the Nicholson analysis^{1a} and ignoring the influence of R_{us} . The solid traces A, B, and C in Figs. 5 and 6 refer to $k_{ob}^s(\text{true})$ values of ∞ , 1.0, and 0.1 cm s^{-1} , respectively. Complete coincidence between these $k_{ob}^s(\text{true})$ values and the corresponding $k_{ob}^s(\text{app})$ values in these plots is only observed when $R_{us} = 0$. A sweep rate of 20 V s^{-1} is used in these simulations, although similar results were obtained at least over the range $1 \leq \nu \leq 100 \text{ V s}^{-1}$. The remaining conditions in Fig. 5 and 6 are also identical, with $C_{dl} = 20 \mu\text{F cm}^{-2}$, except that the electrode area is taken to be 0.2 and 0.02 cm^2 , respectively, in these two figures. Comparable results to those in Figs. 5 and 6 were also obtained if smaller C_{dl} values, in the range 2-20 $\mu\text{F cm}^{-2}$, were employed. Figure 7 shows such a set of results, obtained for the same conditions as in Fig. 6, but with $C_{dl} = 2 \mu\text{F cm}^{-2}$.

From Fig. 5 we can see that for an electrode area of 0.2 cm^2 a significant distinction between a completely reversible reaction [i.e. where $k_{ob}^s(\text{true}) = \infty$] and that for which $k_{ob}^s(\text{true}) = 1 \text{ cm s}^{-1}$ is only possible for very small R_{us} values ($\leq 3 \text{ ohm}$). In other words, the $k_{ob}^s(\text{app})$

values are independent of $k_{ob}^s(\text{true})$ under these conditions, being virtually indistinguishable for larger R_{us} (Fig. 5), so that no meaningful kinetic data can be extracted if $k_{ob}^s(\text{true}) \geq 1 \text{ cm s}^{-1}$. Also evident from Fig. 5 is that if R_{us} is larger than about 10 ohms, no value for $k_{ob}^s(\text{app})$ could be obtained that is larger than about 0.1 cm s^{-1} , a frequently reported value (e.g. ref. 9). Furthermore, the avoidance of substantial discrepancies between $k_{ob}^s(\text{app})$ and $k_{ob}^s(\text{true})$ when the latter approaches 1 cm s^{-1} requires that only extremely small uncompensated resistances be present. For example, in order to evaluate a $k_{ob}^s(\text{true})$ value of 1 cm s^{-1} to 50% accuracy [i.e. to obtain $k_{ob}^s(\text{app}) > 0.5 \text{ cm s}^{-1}$ under these conditions] it is required that $R_{us} < 2 \text{ ohm}$.

Comparing Fig. 5 and 6 shows that decreasing the electrode area improves somewhat this unfavorable situation. Thus for an electrode area of 0.02 cm^2 (Fig. 6) there is a clear experimental distinction between $k_{ob}^s(\text{app})$ values corresponding to $k_{ob}^s(\text{true})$ values of ∞ and 1 cm s^{-1} (curves A and B) even for moderate R_{us} values (ca. 20 ohms), indicating that some kinetic information would be contained in experimental data gathered under these circumstances. Nevertheless, the $k_{ob}^s(\text{app})$ values in curve B fall markedly below $k_{ob}^s(\text{true})$ under these conditions, so that the corrections necessary to extract the latter from the former are still substantial. The errors involved in evaluating smaller $k_{ob}^s(\text{true})$ values, around 0.1 cm s^{-1} , are relatively small since then $k_{ob}^s(\text{app}) \sim k_{ob}^s(\text{true})$ even for $R_{us} \leq 40 \text{ ohm}$ (Fig. 6). This diminished influence of R_{us} with decreasing electrode area is, however, slightly misleading since the effective solution resistance will increase under these conditions, yielding probable increases in R_{us} .

Comparisons with the Influence of Uncompensated Solution Resistance on Rate Constants Determined Using AC Impedance Measurements

Given that ac voltammetry, particularly employing phase-selective impedance measurements, provides the most common means of evaluating k_{ob}^s other than by using cyclic voltammetry, it is of interest to compare quantitatively the extent to which the utility of these two techniques is impaired by the presence of uncompensated resistance. There is ample reason, however, to expect the nature and extent of the influences of R_{us} upon these two techniques to be significantly different. In the ac voltammetric experiment using a stationary electrode, the principal effect of R_{us} is to force the phase of the ac potential waveform across the double layer to differ from that applied by the potentiostat, yielding errors in the apparent phase angle of the current. While the presence of R_{us} also forces the magnitude of the ac potential waveform across the double layer to differ from that controlled by the potentiostat, this is of little consequence since it is generally only the phase angle, rather than the magnitude, of the current which is of relevance to the evaluation of standard rate constants.

The error introduced into the evaluation of k_{ob}^s by ac voltammetry therefore depends principally on the combined influence of R_{us} and the double-layer capacitance, and is diminished with decreasing electrode area to the extent that the total capacitance is also decreased. The effects of R_{us} on cyclic voltammetry have distinctly different origins, as discussed above. Although the extent of the error in evaluating k_{ob}^s with cyclic voltammetry also decreases with the electrode area, this arises primarily as a result of the decreased total current flowing through the cell.

As a consequence, we elected to compare simulated values of $k_{ob}^s(\text{app})$ obtained from phase-selective ac impedance as well as cyclic voltammetry by using conventional data analyses for the following three conditions: (a) electrode area $A = 0.2 \text{ cm}^2$, $C_{dl} = 20 \mu\text{F cm}^{-2}$; (b) $A = 0.02 \text{ cm}^2$, $C_{dl} = 20 \mu\text{F cm}^{-2}$; (c) $A = 0.02 \text{ cm}^2$, $C_{dl} = 2 \mu\text{F cm}^{-2}$. The first two cases span the range of areas commonly encountered with these two techniques, while the second and third cases cover the typical range of capacitance values. The frequency range taken for the ac voltammetric data was between 100 and 500 Hz, the analysis utilizing the frequency dependence of the quadrature to in-phase current ratio, I_Q/I_I (see ref. 6b for simulation details). The resulting plots of $\log k_{ob}^s$ versus R_{us} obtained with ac voltammetry for cases a, b, and c are shown as the dashed curves in Figs. 5, 6, and 7, respectively, to be compared with the solid curves in each of these figures which (as already noted) show corresponding results obtained with cyclic voltammetry. (As noted above, the three $\log k_{ob}^s - R_{us}$ curves in each of these figures labeled A, B, and C, refer to $\log k_{ob}^s(\text{true})$ values of ∞ , 1.0 and 0.1 cm s^{-1} , respectively).

For the large (0.2 cm^2) electrode (Fig. 5), the degree to which $k_{ob}^s(\text{app})$ falls below $k_{ob}^s(\text{true})$ for a given R_{us} value is more marked for ac voltammetry than for cyclic voltammetry. In other words, under the specific conditions prescribed by these simulations the degree of error induced in $k_{ob}^s(\text{app})$ by ignoring solution resistance effects, and therefore the extent of the corrections required to extract $k_{ob}^s(\text{true})$ from $k_{ob}^s(\text{app})$, is smaller for cyclic voltammetry than for ac voltammetry. However, for the smaller (0.02 cm^2) electrode having the same double-layer capacitance per unit area ($20 \mu\text{F cm}^{-2}$), the $\log k_{ob}^s(\text{app}) - R_{us}$ curves obtained for the

two techniques are more comparable (Fig. 6). Moreover, the substitution of a smaller double-layer capacitance (Fig. 7) yields slightly superior $\log k_{ob}^s(\text{app}) - R_{us}$ curves for ac as compared with cyclic voltammetry (Fig. 7).

These examples therefore suggest that roughly comparable errors are introduced into cyclic and ac voltammetric measurements of k_{ob}^s under "typical" conditions in the presence of at least small amounts of uncompensated resistance. However, consideration of other factors lead to the latter technique being clearly favored for this purpose. Most importantly, it is crucial to minimize the value of the uncompensated resistance. This can be achieved relatively readily in the ac experiment since a small amplitude waveform having relatively low frequencies (≥ 2000 Hz) is employed. In contrast, in the cyclic voltammetric experiment the abrupt change in the time derivative of the potential which occurs when the scan direction changes is equivalent to the sudden injection of high-frequency "noise", which will result in a dampened oscillation ("ringing") of the current. The avoidance of severe distortion in the i - E profile for the return scan therefore normally requires the presence of significant uncompensated resistance ($> \text{few ohms}$).

In addition, the accurate estimation of R_{us} for a given level of electronic resistance compensation in the ac impedance experiment is relatively straightforward, either by evaluating the quadrature and in-phase currents at potentials well separated from the ac voltammetric wave or by ac measurements in conjunction with a dummy-cell arrangement.^{6a,b} (The same procedures could, of course, be employed to estimate R_{us} for a given set of experimental conditions, including the resistance compensation setting, used in a cyclic voltammetric experiment.) An alternative

approach to evaluate R_{us} is to select a redox couple which under the measurement conditions employed is known to exhibit $k_{ob}^s(\text{true}) \rightarrow \infty$, so that the measured response is necessarily dominated by R_{us} .¹¹ Although this method has obvious merits, the selection of such a redox couple requires careful consideration.^{11,12} In our experience, using a variety of potentiostats of commercial and in-house design, it is difficult to either measure or minimize R_{us} even for ac impedance measurements to much less than 5 ohms or so in typical nonaqueous media. The corresponding minimum R_{us} values attainable in cyclic voltammetric experiments are often substantially larger.

Another advantage of the phase-selective impedance approach is that a distinction between apparent electrochemical irreversibility brought about by the presence of uncompensated resistance rather than by finite electrode kinetics can be made by examining the dependence of the (I_Q/I_I) ratio upon the ac frequency, ω .^{6b} If the former factor is predominant, then the slope of the $(I_Q/I_I) \cdot \omega^{\frac{1}{2}}$ plot will increase with increasing ω , rather than be independent of ω as will be the case when electrode kinetics controls this response.^{6b} This diagnostic situation can be contrasted with the inability, noted above, of achieving a ready distinction between the dominant presence of R_{us} and finite electrode kinetics by varying the sweep rate in cyclic voltammetry.

Some Considerations for Microelectrodes

The virtues of employing electrodes of especially small dimensions, having radii down to (or below) 1 micron (so-called "microelectrodes" or "ultramicroelectrodes") for electrochemical measurements have recently been explored extensively, including preliminary applications to electrode

kinetics.¹⁰ The advantage of such a marked diminution in electrode area can readily be seen by recalling that while the faradaic current decreases with the square of the electrode radius the effective solution resistance only increases in inverse proportion to the radius.^{10a} Clearly, then, in the absence of iR compensation the deleterious influence of solution resistance will be dramatically reduced by employing micro- rather than conventional electrodes. This advantage is, however, offset somewhat by the iR compensation that is much more readily applied with larger electrodes.

Figure 8 shows illustrative plots of $\log k_{ob}^s(\text{app})$ versus $\log k_{ob}^s(\text{true})$ obtained from simulated cyclic voltammograms for several conditions that are typically encountered with microelectrodes. All curves refer to a sweep rate of 1000 V s^{-1} and a double-layer capacitance of $20 \mu\text{F cm}^{-2}$. (This sweep rate was chosen since comparable values are typically employed with microelectrodes and it is sufficiently rapid so to avoid influences from spherical diffusion even at the small electrodes considered here.) The solid traces A-C refer to an electrode diameter of $1 \mu\text{m}$, having R_{us} values of 1×10^5 , 7×10^5 , and $4 \times 10^6 \text{ ohm}$, respectively. These R_{us} values correspond to solution specific resistances, ρ , of 20, 140, and 800 ohm cm , respectively, obtained from the relation¹³ $R_s = \rho/4r$ where r is the radius of a disk electrode, since in the absence of iR compensation R_{us} will equal the solution resistance R_s . These values were chosen since they are appropriate for concentrated aqueous electrolytes,¹⁴ and 0.1M electrolytes in acetonitrile and dichloroethane, respectively.⁹ While there is reasonable agreement between $k_{ob}^s(\text{app})$ and $k_{ob}^s(\text{true})$ for curves A and B at least up to $k_{ob}^s \sim 10 \text{ cm s}^{-1}$, indicating the virtual absence of R_{us}

effects up to this point, for curve C substantial deviations are observed even for markedly smaller rate constants. This illustrates the need to consider resistive effects when evaluating rapid k_{ob}^s values even with extremely small microelectrodes when relatively high resistance media are employed.

The solid curves E-F in Fig. 8 are the corresponding plots obtained for the same electrolyte (i.e. same ρ values) and other conditions as in curves A-C, but for an electrode diameter of 5 μm . This size is more typically employed at the present time in microelectrode experiments utilizing cyclic voltammetry.¹⁰ While reasonable concordance between $k_{ob}^s(\text{app})$ and $k_{ob}^s(\text{true})$ is seen for $k_{ob}^s \lesssim 10 \text{ cm s}^{-1}$ in the least resistive media (curve D), the results obtained for conditions corresponding to typical nonaqueous media (curves E and F) are substantially inferior. Indeed, the 5 μm electrode in dichloroethane shows that $k_{ob}^s(\text{app}) \ll k_{ob}^s(\text{true})$ at least for $k_{ob}^s(\text{true}) > 1 \text{ cm s}^{-1}$; i.e. the ΔE_p values are determined almost entirely by solution resistance effects under these conditions.

Figure 8 also contains a comparative $\log k_{ob}^s(\text{app}) - \log k_{ob}^s(\text{true})$ trace obtained for the conditions of curve E, but utilizing ac rather than cyclic voltammetry in the fashion prescribed above (dashed trace). As for the behavior noted above for the larger size electrodes, the influence of solution resistance upon the ac and cyclic voltammetric response is seen to be similar. Comparable behavior was also obtained for the other conditions considered in Fig. 8.

Concluding Remarks

The foregoing considerations demonstrate that the deleterious influence of uncompensated solution resistance imposes a severe and

sometimes unexpected limitation on the magnitude of standard rate constants that can be evaluated by means of cyclic voltammetry. In order to extract meaningful k_{ob}^s values using this technique, it is clearly imperative to obtain reliable estimates of R_{us} for the measurement conditions employed, and to demonstrate that R_{us} is sufficiently small so that $k_{ob}^s(app)$ approximates $k_{ob}^s(true)$. The observation of $k_{ob}^s(app)$ values that approach the limiting value dictated by the known uncompensated resistance; i.e. those corresponding to $k_{ob}^s(true) \rightarrow \infty$, provides a clear signal that the desired electrode kinetics are not measurable under the conditions employed. Given a reliable knowledge of R_{us} , desired $k_{ob}^s(true)$ values can still be evaluated in the intermediate case of partial kinetic-resistive control from the $k_{ob}^s(app)$ values by using the appropriate $k_{ob}^s(app) - k_{ob}^s(true)$ relation extracted from digital simulations.

Although the extent of the systematic errors in $k_{ob}^s(app)$ values obtained by cyclic and ac voltammetry are surprisingly comparable for typical R_{us} values, the latter technique would seem to exhibit clear advantages for the evaluation of fast electrode kinetics under most conditions. This stems both from the ability to better minimize and evaluate R_{us} with ac impedance measurements, and from the diagnosis of dominant resistive effects from the observation of nonlinear $(I_Q/I_I) - \omega^2$ plots.

As has already been well documented,¹⁰ the use of cyclic voltammetry with microelectrodes offers real advantages for evaluating standard rate constants. However, even under these conditions the influence of cell resistance can provide a serious impediment to the evaluation of k_{ob}^s values greatly in excess of 1 cm s^{-1} , especially for high resistance media and in

the absence of iR compensation. It therefore would appear that k_{ob}^s values evaluated by any of these approaches, especially for moderately fast reactions ($k_{ob}^s \geq 0.1 \text{ cm s}^{-1}$) should be regarded with some skepticism in the absence of due consideration of solution resistance effects by the experimenter.

Acknowledgment

This work is supported by the Office of Naval Research.

References

1. (a) R. S. Nicholson, Anal. Chem., 37 (1965), 1351; (b) R. S. Nicholson and I. Shain, Anal. Chem., 36 (1964), 706.
2. (a) J. M. Saveant and D. Tessier, J. Electroanal. Chem., 65 (1975), 57; (b) J. M. Saveant and D. Tessier, J. Electroanal. Chem., 77 (1977), 225; (c) K. B. Oldham, J. Electroanal. Chem., 72 (1976), 371; (d) P. E. Whitson, H. W. VandenBoren, and D. H. Evans, Anal. Chem., 45 (1973), 1298; (e) B. Aalstad and V. D. Parker, J. Electroanal. Chem., 122 (1981), 183; (f) B. Speiser, Anal. Chem., 57 (1985), 1390.
3. S. W. Feldberg, in "Electroanalytical Chemistry - A Series of Advances", A. J. Bard, ed., M. Dekker, New York, Vol. 3, 1969, p. 199.
4. (a) R. S. Nicholson, Anal. Chem., 37 (1965), 667; (b) W. T. DeVries and E. VanDalen, J. Electroanal. Chem., 10 (1965), 183.
5. (a) D. Garreau and J.-M. Saveant, J. Electroanal. Chem., 86 (1978), 63; (b) D. F. Milner, Ph.D. thesis, Purdue University, 1987.
6. (a) D. F. Milner and M. J. Weaver, J. Electroanal. Chem., in press; (b) D. F. Milner and M. J. Weaver, J. Electroanal. Chem., 191 (1985), 411.
7. D. A. Corrigan and D. H. Evans, J. Electroanal. Chem., 106 (1980), 287.
8. V. D. Parker, "Electroanalytical Chemistry - A Series of Advances", A. J. Bard, ed., Vol. 14, M. Dekker, New York, 1986, p. 1.
9. K. M. Kadish, J. Q. Ding and T. Malinski, Anal. Chem., 56 (1984), 1741.
10. (a) J. O. Howell and R. M. Wightman, Anal. Chem., 56 (1984), 524; (b) J. O. Howell and R. M. Wightman, J. Phys. Chem., 88 (1984), 3915; (c)

- M. I. Montenegro and D. Pletcher, J. Electroanal. Chem., 200 (1986), 371; (d) A. M. Bond, T. L. E. Henderson, and W. Thormann, J. Phys. Chem., 90 (1986), 2911.
11. T. Gennett and M. J. Weaver, Anal. Chem., 56 (1984), 1444.
 12. G. E. McManis, M. N. Golovin, and M. J. Weaver, J. Phys. Chem., 90 (1986), 6563.
 13. J. Newman, J. Electrochem. Soc., 113 (1966), 501.
 14. J. F. Chambers, J. Phys. Chem., 62 (1958), 1136.

Figure Captions

Fig. 1

Comparison between a simulated current-potential curve for a linear-sweep voltammogram (A) and the corresponding time derivative of the potential across the double layer, dE_{dl}/dt (B). Simulation conditions are: reactant concentration $C_b = 1\text{mM}$; electrode area $A = 0.2\text{ cm}^2$, diffusion coefficient $D = 1 \times 10^{-5}\text{ cm s}^{-1}$; sweep rate $\nu = 100\text{ V s}^{-1}$, uncompensated resistance $R_{us} = 50\ \Omega$, double-layer capacitance, $D_{dl} = 20\ \mu\text{F cm}^{-2}$, true standard rate constant, $k_{ob}^s(\text{true}) = \infty$.

Fig. 2

Illustrative comparison of the simulated effects of uncompensated solution resistance and finite electrode kinetics on cyclic voltammograms. Solid trace is for $C_b = 1\text{mM}$, $\nu = 20\text{ V s}^{-1}$, $C_{dl} = 0$, $D = 1 \times 10^{-5}\text{ cm s}^{-1}$, $A = 0.2\text{ cm}^2$, $R_{us} = 0$, and $k_{ob}^s(\text{true}) = 0.04\text{ cm s}^{-1}$. Squares are obtained for the same conditions, but for $R_{us} = 50\ \Omega$ and $k_{ob}^s(\text{true}) = \infty$.

Fig. 3

Illustrative comparison of the simulated effects of uncompensated solution resistance (squares) and finite electrode kinetics (solid trace) on cyclic voltammetric potential peak separations, ΔE_p , as a function of sweep rate, ν . Simulation conditions as in Fig. 2.

Fig. 4

Dependence of cyclic voltammetric potential peak separation, ΔE_p , upon reactant concentration C_b in the presence of uncompensated solution resistance, R_{us} . R_{us} values are A, 50 Ω ; B, 20 Ω ; C, 5 Ω . Other simulation conditions are: $k_{ob}^s(\text{true}) = \infty$, $\nu = 20 \text{ V s}^{-1}$, $C_{dl} = 20 \mu\text{F cm}^{-2}$, $D = 1 \times 10^{-5} \text{ cm}^2 \text{ s}^{-1}$, $A = 0.2 \text{ cm}^2$.

Fig. 5

Plots of $\log k_{ob}^s(\text{app})$, where $k_{ob}^s(\text{app})$ is the "apparent" rate constant extracted from simulated cyclic voltammograms (solid traces) or ac voltammograms (dashed traces) assuming $R_{us} = 0$, against R_{us} for various values of the actual ("true") rate constant, $k_{ob}^s(\text{true})$. Curves A, B, and C are for $k_{ob}^s(\text{true}) = \infty$, 1, and 0.1 cm s^{-1} , respectively. Other simulation conditions are $C_b = 1 \text{ mM}$, $C_{dl} = 20 \mu\text{F cm}^{-2}$, $A = 0.2 \text{ cm}^2$, $D = 1 \times 10^{-5} \text{ cm}^2 \text{ s}^{-1}$. The cyclic voltammetric sweep rate is 20 V s^{-1} , and the ac impedance data are for frequencies between 100 and 500 Hz (see text for further details).

Fig. 6

As for Fig. 5, but for an electrode area, A , of 0.02 cm^2 .

Fig. 7

As for Fig. 6, but for a double-layer capacitance, C_{dl} , of $2 \mu\text{F cm}^{-2}$.

Fig. 8

Illustrative relationships between $k_{ob}^s(\text{app})$ and $k_{ob}^s(\text{true})$ for some typical conditions encountered with cyclic voltammetry using microelectrodes. Curves A-C and D-F are for 1.0 and 5 μm diameter electrodes, respectively. Key to solution resistance conditions: A, $R_{us} = 10^5 \Omega$ ($\rho = 20 \Omega \text{ cm}$); B, $R_{us} = 7 \times 10^5 \Omega$ ($\rho = 140 \Omega \text{ cm}$); C, $R_{us} = 4 \times 10^6 \Omega$ ($\rho = 800 \Omega \text{ cm}$); D, $R_{us} = 2 \times 10^4 \Omega$ ($\rho = 20 \Omega \text{ cm}$); E, $R_{us} = 10^5 \Omega$ ($\rho = 140 \Omega \text{ cm}$); F, $R_{us} = 7 \times 10^5 \Omega$ ($\rho = 800 \Omega \text{ cm}$). Other simulation conditions are $C_d = 1 \text{ mF}$, $\nu = 1000 \text{ V s}^{-1}$, $C_{dl} = 20 \mu\text{F cm}^{-2}$, $D = 1 \times 10^{-5} \text{ cm}^2 \text{ s}^{-1}$. The dashed curve is from a simulation corresponding to curve E, but obtained for ac impedance data taken between ac frequencies of 100-500 Hz.

FIG 1

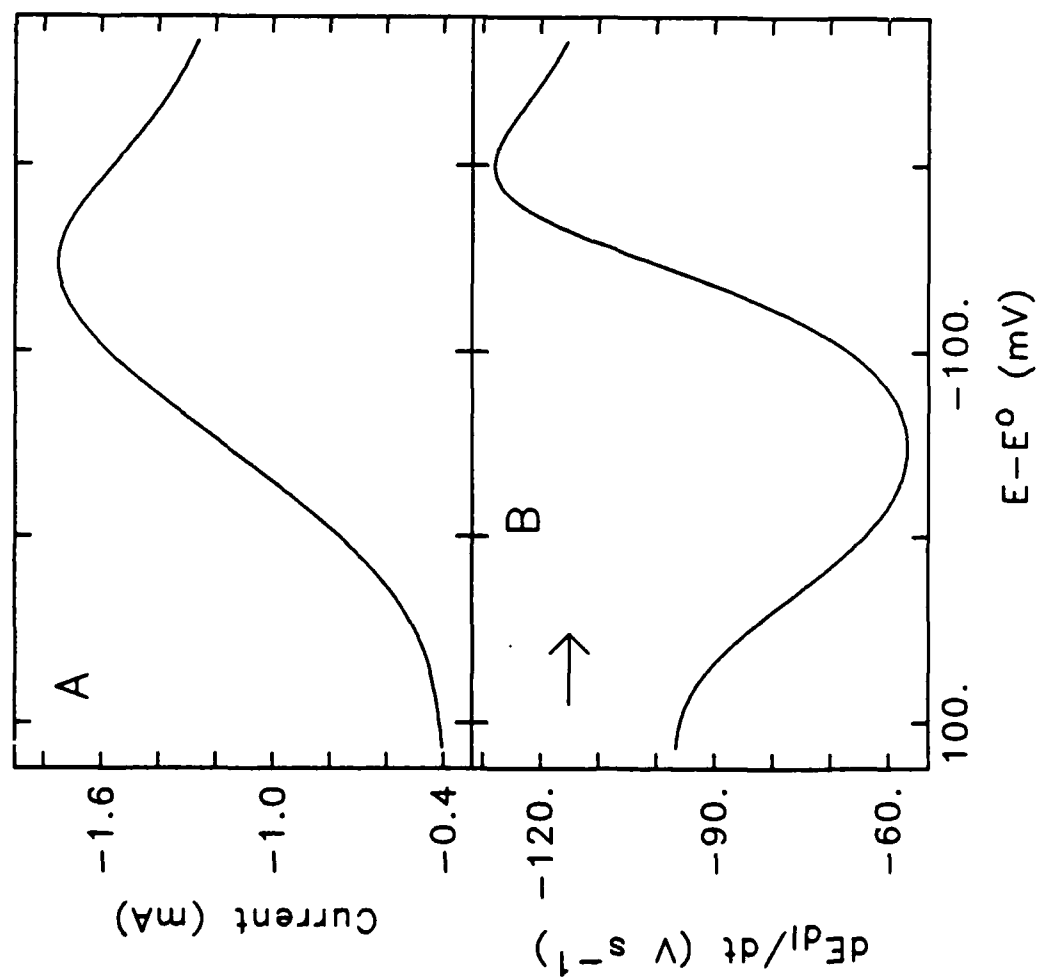


FIG 2

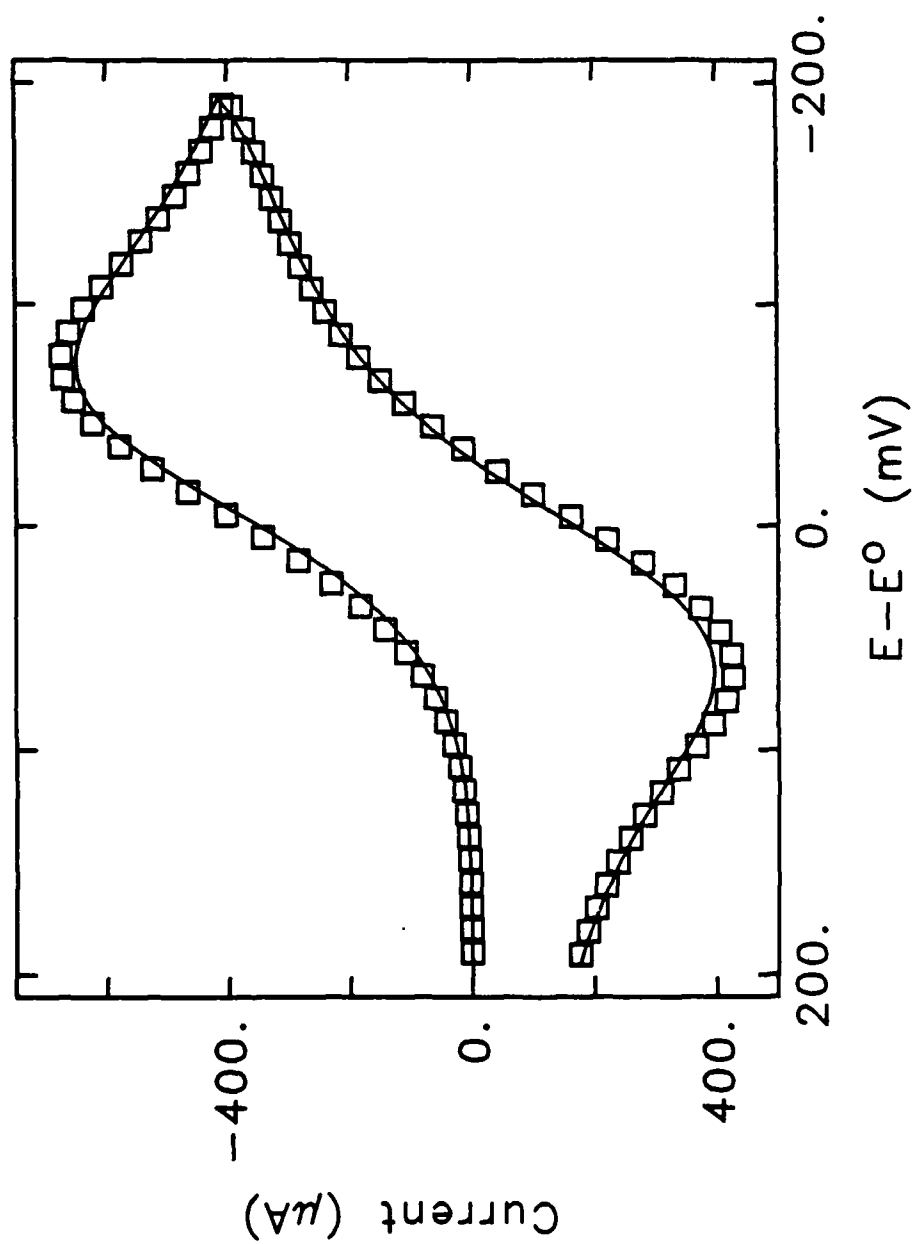


FIG 3

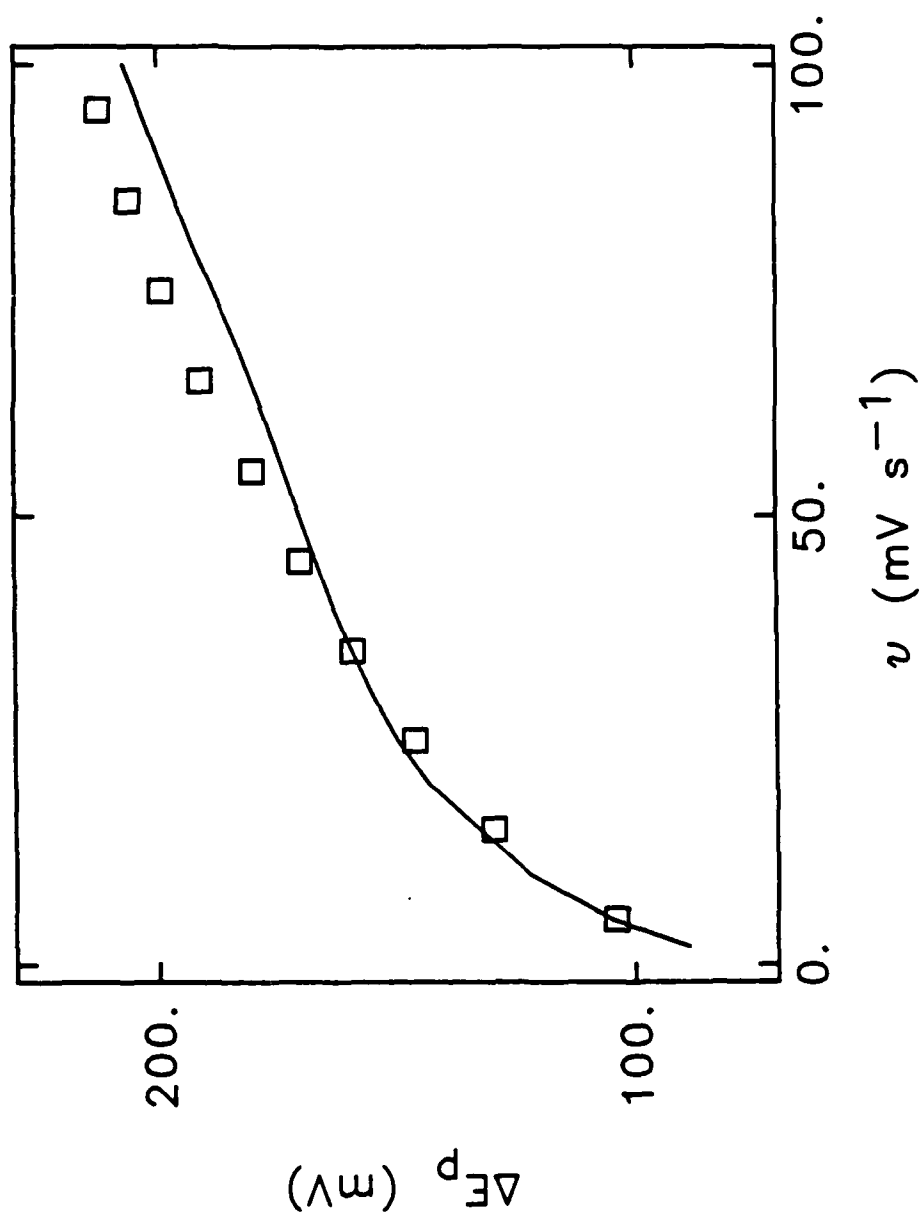


FIG 4

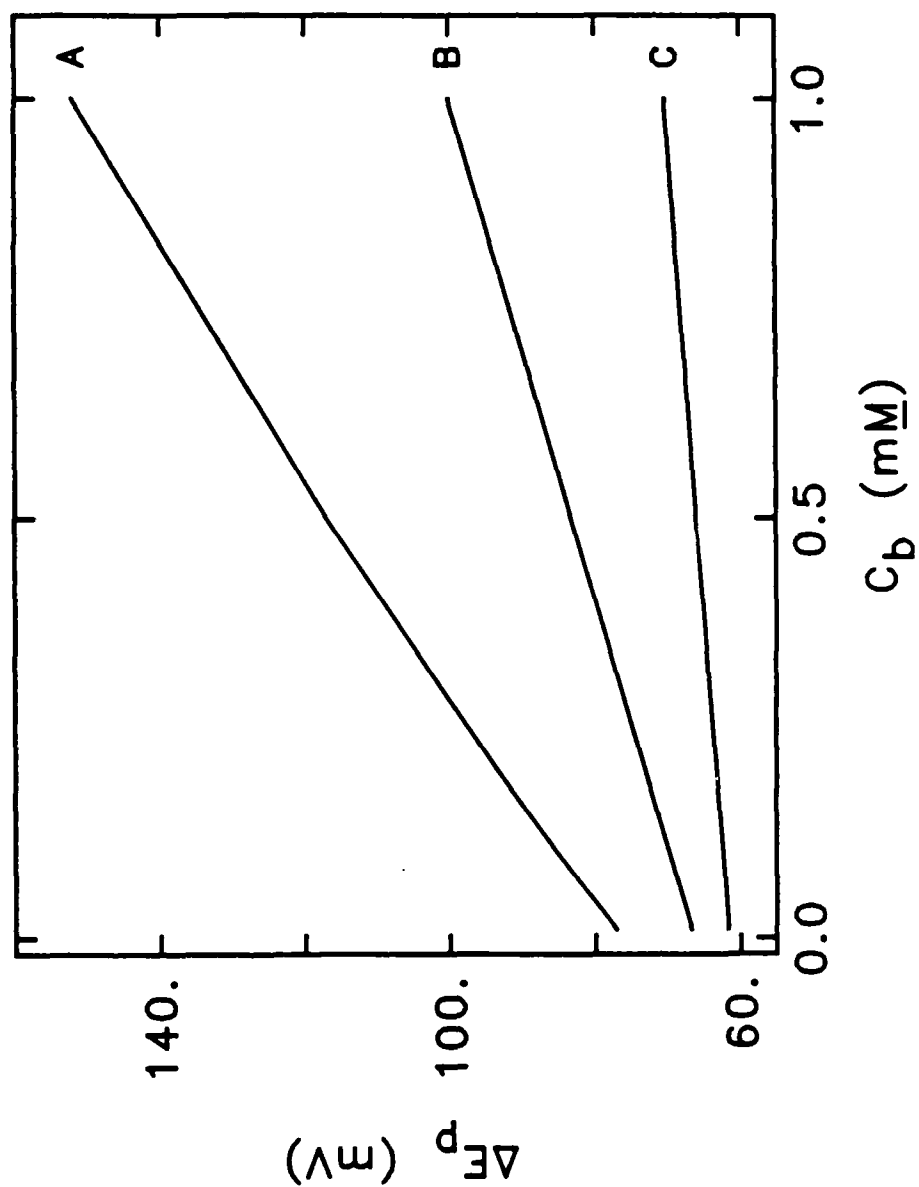


Fig 5

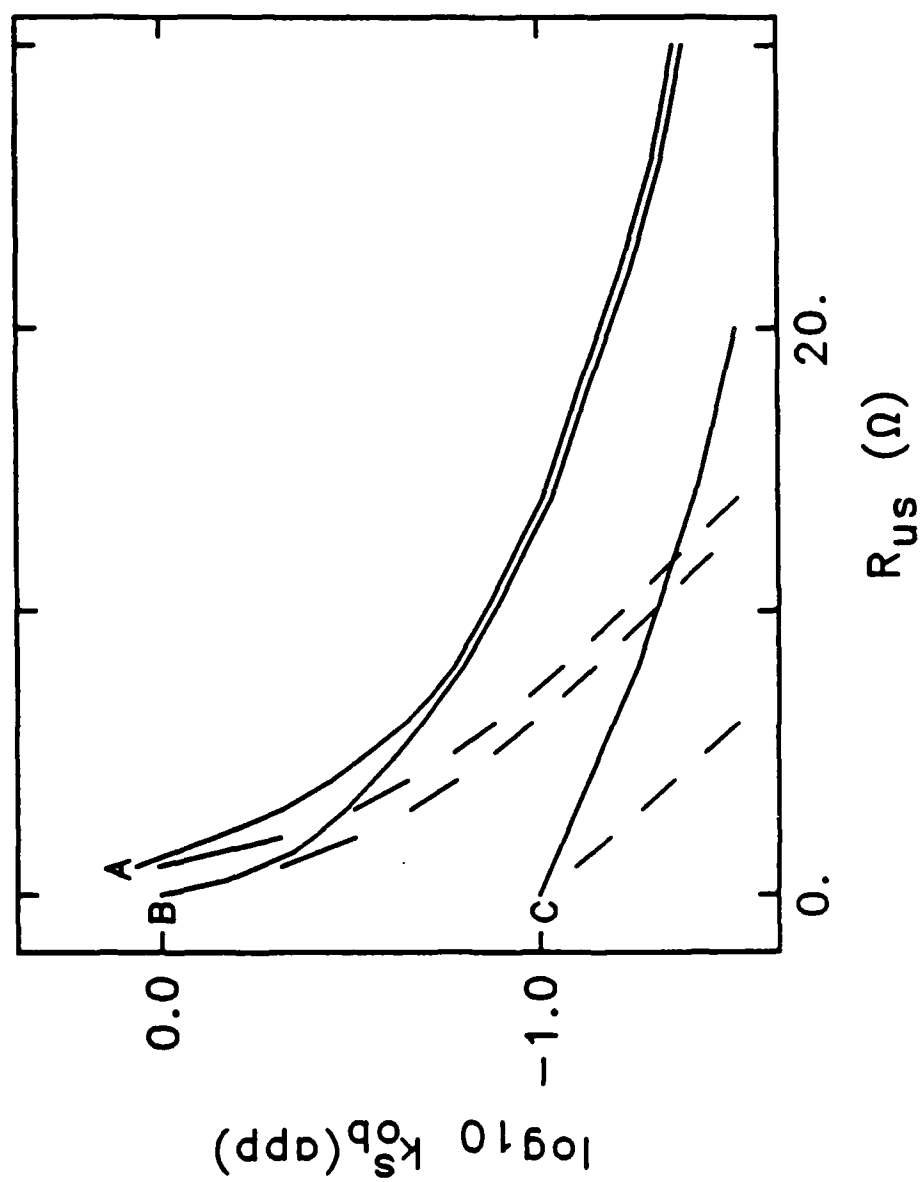


FIG 6

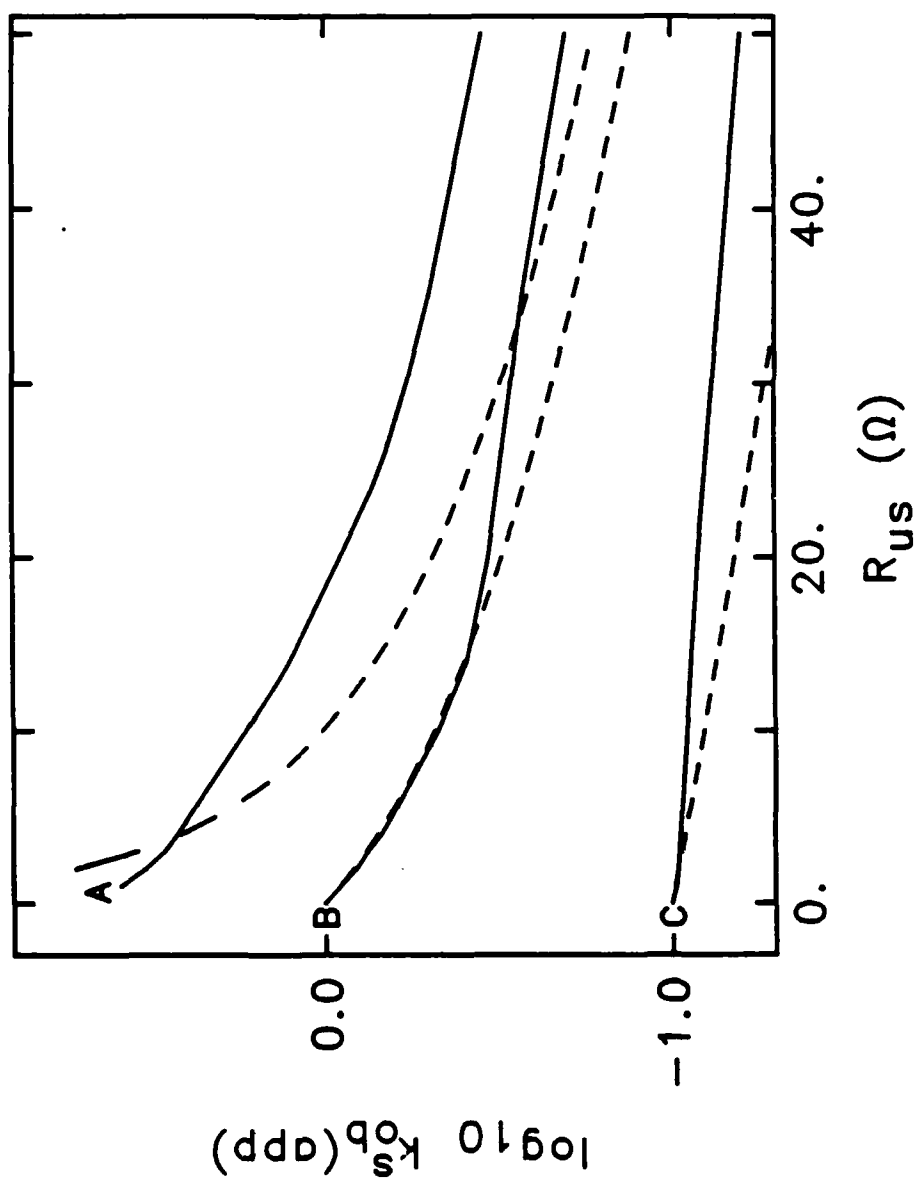


FIG 7

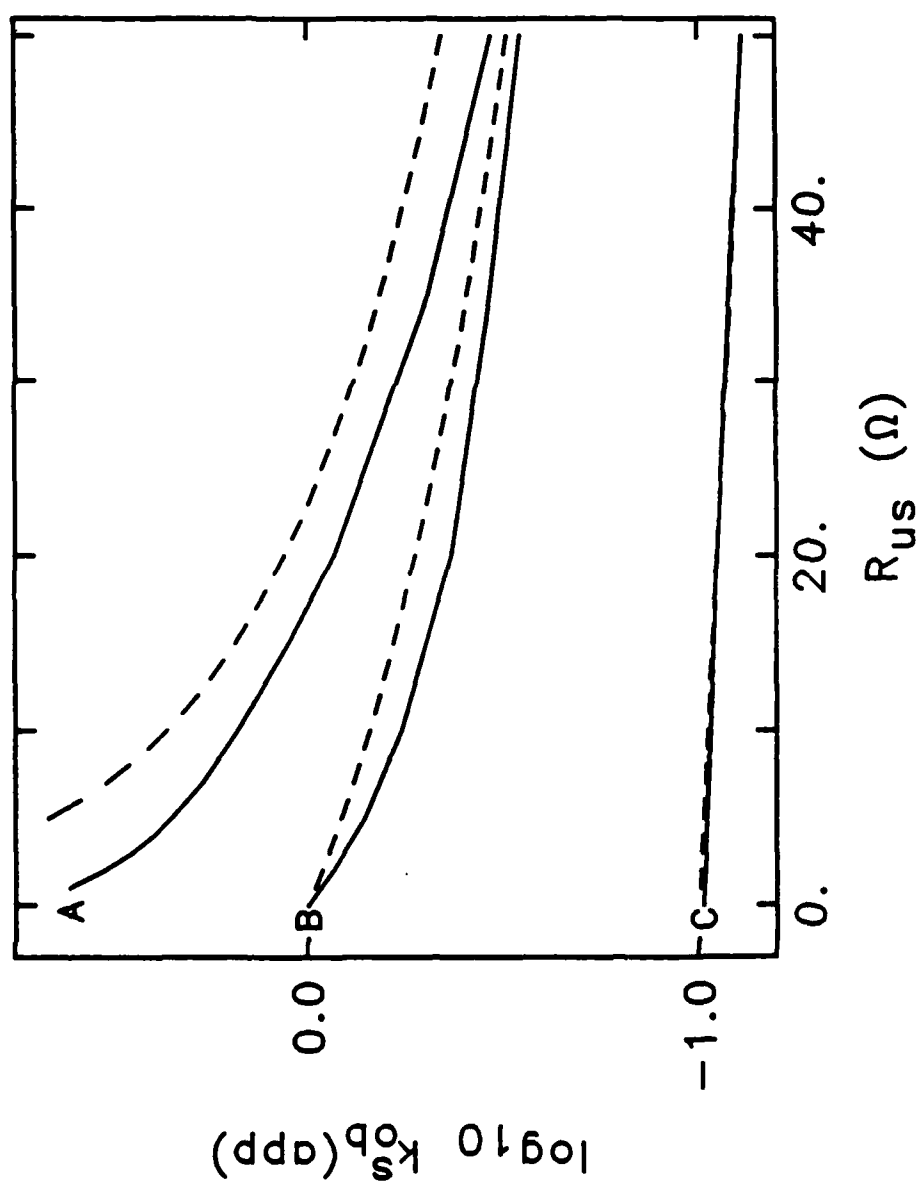
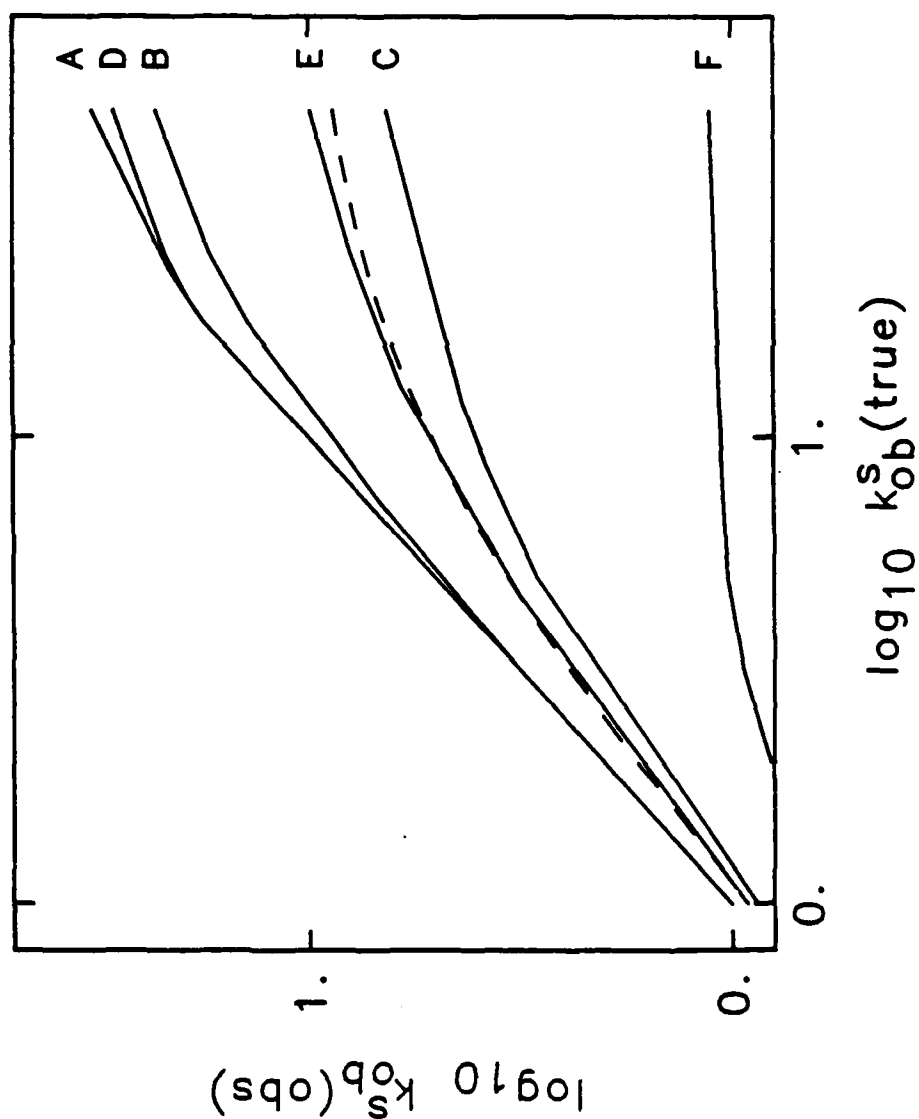


FIG 8



END

DATE

FILMED

6-1988

DTic